Title
THz micro-Doppler measurements based on a silicon-based Picosecond pulse radiator

Author
Razavian, Sam

Publication Date
2019-05-07

Peer reviewed

THz Micro-Doppler Measurements Based On A Silicon-Based Picosecond Pulse Radiator

Sam Razavian, M. Mahdi Assefzadeh, Mostafa Hosseini, Aydin Babakhani
University of California, Los Angeles, CA 90095, USA

***Abstract*— In this paper, a custom picosecond pulse radiator is used to demonstrate the micro-Doppler phenomenon in the Terahertz (THz) regime. In the micro-Doppler effect, the periodic movement of radar targets modulates the frequency of the electromagnetic waves reflected from their surface. The modulation depth is dependant on the intensity of the vibrations and the carrier frequency. Therefore, using carrier tones in the THz regime enables detection of weak micro-Doppler signatures. In this experiment, sound vibrations with frequency of 50 to 700 Hz were used to modulate a 395.2 GHz carrier signal produced by a digital-to-impulse (D2I) silicon chip. A ten-second music track, a chirp sound, and multiple frequency tones were produced by a speaker and then were reconstructed through the micro-Doppler effect. The sound waves were recovered via frequency demodulation at the receiver.**

***Keywords*— D2I, Doppler, depth of modulation, FM, micro-Doppler, radar, terahertz, THz source**

I. Introduction

The Doppler effect has been widely used in radar engineering to measure the speed of moving objects such as drones and airplanes. Similarly, the micro-Doppler phenomenon, which roots from the Doppler effect, is used to detect the micro-motion signatures of objects. This effect has been used to characterize, identify, and distinguish moving objects [1]. In [2], the frequency of heart beat is measured using an ultra-wide band radar. In [3], a 160-GHz radar is used to sense throat vibrations and reconstruct the speech.

Moreover, micro-Doppler phenomenon can be used for wireless detection of sound. Mechanical sound waves can cause micro-vibrations on the surface of an object. The surface micro-vibrations can shift (modulate) the frequency of the incident electromagnetic waves. Hence, by demodulating and processing the reflected waves, the original sound can be recovered. In this paper, we have shown vibrations caused by sound modulate the frequency of the reflected waves and how we can recover the original sound using frequency demodulation.

In section II, we review the theory of Frequency Modulation (FM) caused by sound vibrations. Section III describes the details of the experimental setup. In section IV, the micro-Doppler measurement results are discussed and section V concludes this paper. In this work, we have used a Digital-to-Impulse (D2I) chip reported in [4] to radiate THz tones. This chip produces frequency comb from 30 GHz to 1.1 THz with programmable spacing set by the repetition rate of the input trigger.

II. micro-Doppler Analysis

Fig. 1 illustrates the micro-Doppler effect on the reflected beam from a surface that vibrates with an angular velocity of ω_s. The reflected signal can be expressed as

$$R(t) = A\cos\left(2\pi f_c t + 2\pi\int f_d(t)dt\right) \tag{1}$$

and

$$f_d(t) = \frac{2v(t)\cos(\theta)}{c} f_c \tag{2}$$

$$v(t) = D\omega_s \cos(\omega_s t) \tag{3}$$

where $f_d(t)$ is the instantaneous frequency shift, f_c is the carrier frequency (frequency of the tone), $v(t)$ is the instantaneous velocity of the reflecting surface, D is the amplitude of the vibration, c is the velocity of the electromagnetic wave, and θ is the angle between the vibration direction and the incident wave. (1) can be expanded in the following explicit form:

$$\begin{aligned} R(t) &= A\cos\left(\omega_c t + \frac{2D\cos(\theta)\omega_c}{c}\sin(\omega_s t)\right) \\ &= A\sum_{k=-\infty}^{\infty} J_k(\beta)\cos\left((\omega_c + k\omega_s)t\right) \end{aligned} \tag{4}$$

where J is the Bessel function and β is the modulation index (modulation depth) of the FM modulation, which is directly proportional to the carrier frequency. Hence, by increasing the carrier frequency, a larger modulation depth and a wider bandwidth is achieved.

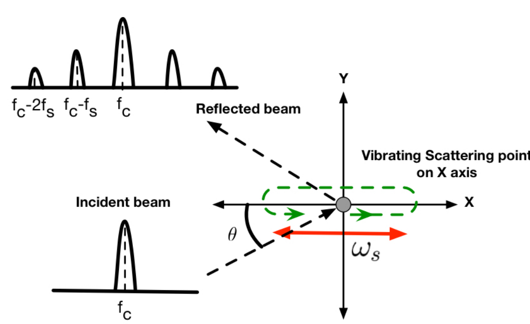

Fig. 1. FM modulation because of the micro-Doppler

Another key factor that determines the lower limit of the detectable vibration frequency and overall quality of the recovered sound is the linewidth of the carrier frequency tone. A narrow spectral linewidth is necessary for the detection of low-frequency vibrations. Particularly, this issue is more critical at millimeter-wave and THz frequencies, where oscillator-based radiators suffer from poor phase noise and frequency instability. In D2I architecture, the frequency of the radiated tones is locked to the input trigger. As a result, the phase noise of the radiated tones is set by the input trigger. This means that by using a low-phase-noise input trigger, the spectral linewidth can be minimized.

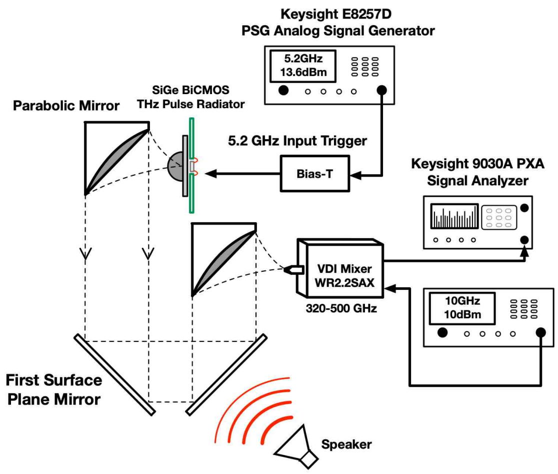

Fig. 2. Measurement setup for modulation and demodulation of sound waves using micro-Doppler effect

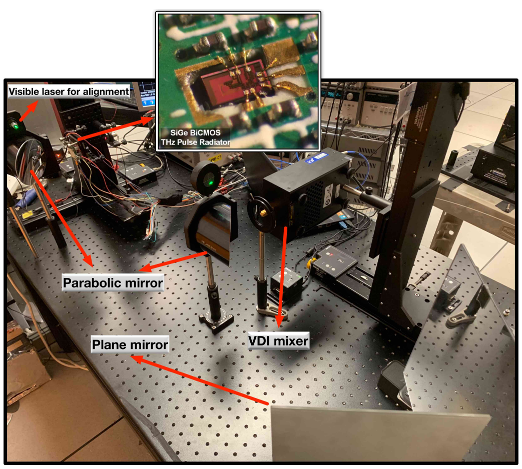

Fig. 3. Experimental setup used for modulation and demodulation of sound waves

III. Experimental Setup

A SiGe BiCMOS picosecond pulse generator with an on-chip antenna is used as the radiating source in this experiment. This chip radiates 1.9-ps pulses with a repetition rate of 5.2 GHz. In the frequency domain, the chip radiates an ultra-stable frequency comb with a center frequency of 160 GHz and a 3dB-BW of 130 GHz.

Due to the high dielectric constant of silicon substrate, the radiation of the on-chip antenna is coupled to the substrate modes. Hence, a hemispherical silicon lens is placed on the back of the chip to eliminate the substrate modes and increase the total radiation efficiency.

As discussed in the previous section, the narrow linewidth of the carrier tone can improve the SNR of micro-Doppler signatures. In this experimental setup, THz tones with a 10-dB linewidth of 2 Hz are radiated.

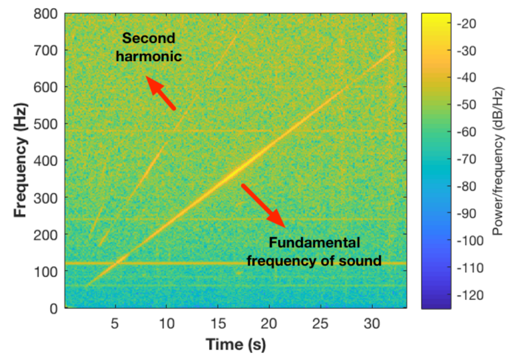

Fig. 4. Spectrogram of a recovered 30-sec chirp sound

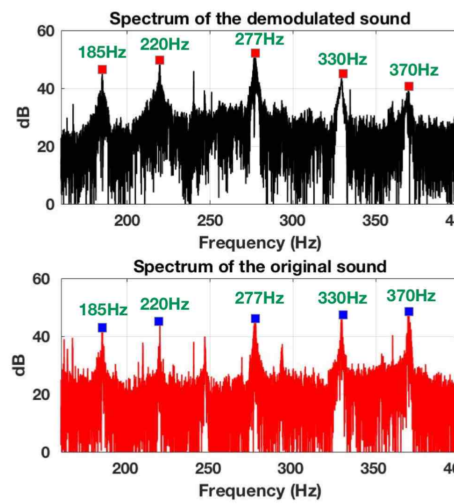

Fig. 5. Comparison between the demodulated sound and the original sound track

Fig. 2 shows a diagram of the measurement setup. A picture of the measurement setup is also shown in Fig. 3. Off-axis parabolic mirrors were used to collimate the THz radiation at the transmitter and focus it on the horn antenna on the receiver side. Two plane mirrors were used to direct the collimated beam and pick up the mechanical sound vibrations from the speaker. A precise alignment is important to maximize the received THz power. The alignment was performed with the aid of a visible light laser. A 1-mW visible laser was used to precisely align the D2I chip and mirrors (Fig. 3). On the receiver side, a VDI Spectrum Analyzer Exetender (SAX) in the 320-500 GHz band was used to down-convert the received signal, in conjunction with a Keysight PXA9030N signal analyzer. The same signal analyzer was also used to demodulate the micro-Doppler FM signal and recover the sound.

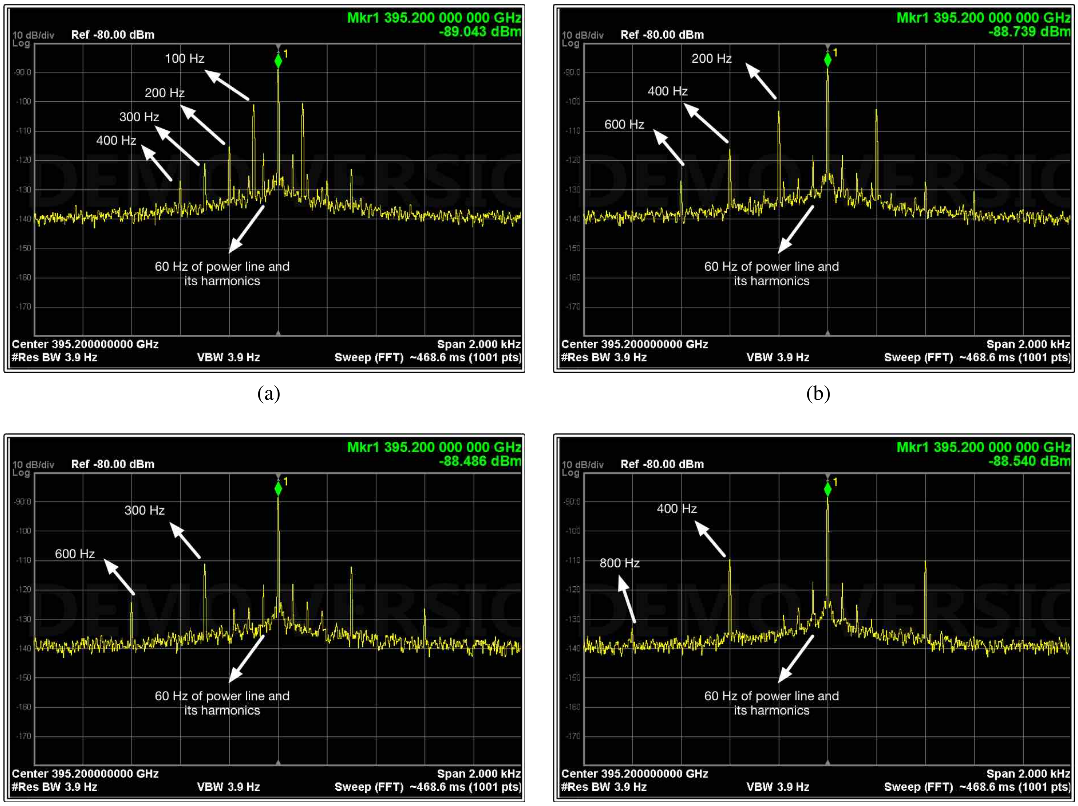

(a) (b) (c) (d)

Fig. 6. FM modulation for four different sound tones: (a) 100Hz, (b) 200Hz, (c) 300Hz, (d) 400Hz

IV. Measurement Results

A THz tone at 395.2 GHz with a measured power of −88.5 dBm at the receiver was chosen as the carrier. In the first experiment, a 10-sec music track and a 30-sec chirp audio signal (50 to 700 Hz) were played via a speaker in the proximity of the plane mirror (Fig. 2). The sound was recovered at the receiver from the micro-Doppler signatures of the plane mirror. To avoid loss of information, the recovered sound must preserve the main frequency components of the original sound waves. Fig. 4 shows that fundamental frequency components of the recovered sound follow the original chirp sound. Additionally, In Fig. 5, the frequency spectrum of both the original music track and the reconstructed version are compared. It's explicit that the frequency peaks in the spectrum of the original track match with the peaks in the recovered sound.

To demonstrate the frequency modulation of the carrier tone, single frequency tones at 100 Hz, 200 Hz, 300 Hz, and 400 Hz were produced by the speaker. As shown in Fig. 6, the FM tones can be seen around the carrier frequency with the spacing set by the frequency of the sound vibration. As the sound frequency increases, the FM tones becomes weaker. This effect is mostly due to the lower coupling of the mechanical sound waves to the surface of the mirror at higher frequencies. The spurious 60-Hz tones and their harmonics shown in the spectrum are caused by the coupling of the power line.

V. Conclusion

This paper demonstrates the micro-Doppler phenomenon at THz frequencies. An experimental setup was designed and utilized to retrieve sound waves using micro-Doppler effect. The micro-Doppler signature of a scattering surface was recorded using a THz carrier tone generated by a custom THz impulse radiator chip. Due to higher modulation depth, which is achieved by using THz carrier tones, micro-Doppler signatures were recorded with high SNR. Additionally, narrow spectral linewidth of the tones enabled detection of vibrations with a frequency as low as 50 Hz. The approach of this paper allows us to detect the subtle micro-doppler signature of scattering surfaces wirelessly using a tiny THz radiator chip.

References

[1] X. Bai, F. Zhou, M. Xing, and B. Zheng, "Micro-doppler analysis and imaging of air-planes with rotating parts," *2009 2nd Asian-Pacific Conference on Synthetic Aperture Radar*, pp. 610–613, 2009.

[2] L. Ren, Y. S. Koo, Y. Wang, and A. E. Fathy, "Noncontact heartbeat detection using uwb impulse doppler radar," *2015 IEEE Topical Conference on Biomedical Wireless Technologies, Networks, and Sensing Systems (BioWireleSS)*, pp. 1–3, 2015.

[3] M. Geiger, D. Schlotthauer, and C. Waldschmid, "Improved throat vibration sensing with a flexible 160-ghz radar through harmonic generation," *2018 IEEE/MTT-S International Microwave Symposium - IMS*, pp. 123–126, Jun. 2018.

[4] M. M. Assefzadeh and A. Babakhani, "Broadband oscillator-free thz pulse generation and radiation based on direct digital-to-impulse architecture," *IEEE J. Solid-State Circuits*, vol. 52, no. 15, pp. 1244–1245, Nov. 2017.